

SUPERNOVAE

A transient radio source consistent with a merger-triggered core collapse supernova

D. Z. Dong^{1*}, G. Hallinan¹, E. Nakar², A. Y. Q. Ho^{1,3,4}, A. K. Hughes⁵, K. Hotokezaka⁶, S. T. Myers⁷, K. De¹, K. P. Mooley^{1,7}, V. Ravi¹, A. Horesh⁸, M. M. Kasliwal¹, S. R. Kulkarni¹

A core collapse supernova occurs when exothermic fusion ceases in the core of a massive star, which is typically caused by exhaustion of nuclear fuel. Theory predicts that fusion could be interrupted earlier by merging of the star with a compact binary companion. We report a luminous radio transient, VT J121001+495647, found in the Very Large Array Sky Survey. The radio emission is consistent with supernova ejecta colliding with a dense shell of material, potentially ejected by binary interaction in the centuries before explosion. We associate the supernova with an archival x-ray transient, which implies that a relativistic jet was launched during the explosion. The combination of an early relativistic jet and late-time dense interaction is consistent with expectations for a merger-driven explosion.

Most massive stars [i.e., those more massive than eight solar masses (M_{\odot})] are born in close binaries, within which expansion of one star during its evolution can lead to mass transfer with the companion (1, 2). In some systems, the faster-evolving (more massive) star explodes as a supernova, leaving behind a compact object (neutron star or black hole) remnant in a close orbit with its companion. When the companion (second star) later expands, it transfers mass in the other direction, onto the compact object. Systems of this type with wide orbits have been observed in the Milky Way (3). Those with closer orbits undergo unstable mass transfer, causing the compact object to spiral into the atmosphere of the massive star, forming a common envelope binary.

During the common envelope phase, the outer atmosphere of the donor star becomes unbound, forming a dense and expanding toroidal shell around the binary (4). The physics of the common envelope are difficult to model. Some inspirals halt before reaching the donor's core. This process is a leading candidate for producing the close double-compact-object binaries detected by gravitational wave observatories (5). Other systems are expected to spiral inward until the compact object reaches the star's core. Theory predicts that some of these systems tidally disrupt the core, forming a rapidly accreting, neutrino-cooled disk (6). This energetic accretion is predicted to

launch a jet and cause a merger-driven explosion (6–8).

We performed a systematic blind search for radio transients in the Very Large Array Sky Survey (VLASS) (9). We identified and followed up luminous point sources associated with galaxies closer than 200 megaparsec (Mpc) that are present in the first half-epoch (Epoch 1.1; September 2017 to February 2018) of the survey but absent from the earlier (1994–2005) Faint Images of the Radio Sky at Twenty-Centimeters (FIRST) survey (10, 11). The most luminous source that we identified was VLASS transient J121001+495647 (hereafter abbreviated VT 1210+4956), located in an off-nuclear region of the dwarf star-forming galaxy SDSS J121001.38+495641.7 (Fig. 1) (12). This galaxy has a stellar mass of $\sim 10^{9.2} M_{\odot}$, a specific star formation rate of $\sim 0.25 M_{\odot} \text{ Gyr}^{-1} M_{\odot}^{-1}$, and an abundance of elements heavier than helium (metallicity) of $\sim 80\%$ the solar value (12).

We observed two follow-up epochs with the Karl G. Jansky Very Large Array (VLA), finding a peak radio luminosity of $1.5 \times 10^{29} \text{ erg s}^{-1} \text{ Hz}^{-1}$ at 5 GHz (Fig. 1) (11), 10 times more luminous than any other non-nuclear transient found in our search. We obtained an optical spectrum of the radio transient location using the Low Resolution Imaging Spectrometer on the Keck I telescope, which exhibits a hydrogen-alpha (H α at 6563Å) emission line with luminosity $(7.3 \pm 0.3) \times 10^{38} \text{ erg s}^{-1}$ and full width at half maximum of $\sim 1340 \pm 60 \text{ km s}^{-1}$ (Fig. 2) (11). This emission line implies a massive, ionized outflow associated with the radio source (13, 14), and its redshift $z = 0.03470 \pm 0.00003$ confirms its association with the host galaxy, which is at $z = 0.03472 \pm 0.00003$ (12). In addition to the broad component, we observed spectrally unresolved (narrow) emission lines consistent with a co-located star-forming region. The environment, broad line, and high radio luminosity indicate a likely association with the explosion of a massive star.

Radio emission from supernovae is powered by synchrotron emission from fast ejecta driving a shock into the ambient circumstellar medium (CSM) (15). The most luminous events require exceptionally fast material, such as relativistic (close to the speed of light) jets driven by central compact-object engines or interaction with a particularly dense CSM. All known supernovae with radio emission peaking at $\geq 10^{29} \text{ erg s}^{-1} \text{ Hz}^{-1}$ are high-luminosity examples of transient classes that involve central engines (e.g., 16–21). Supernovae featuring dense CSM interaction are typically more than an order of magnitude less luminous. Given the high luminosity of VT 1210+4956, we checked for early-time signatures of a central engine by searching archival optical, x-ray, and gamma-ray transient catalogs for a counterpart source (11). This search yielded one match: gamma-ray burst (GRB) 140814A, an unusual soft x-ray burst detected by the Monitor of All Sky X-ray Image (MAXI) instrument on the International Space Station using its Gas Slit Camera (GSC) (22).

GRB 140814A was detected by the GSC at 2 to 4 keV and 4 to 10 keV in a $15 \pm 3 \text{ s}$ window centered at 07:12:23 Universal Time on 14 August 2014, with a similar flux in both bands. It was not detected in a simultaneous observation with a similar sensitivity in the GSC 10- to 20-keV band, suggesting a characteristic energy of $\sim 5 \text{ keV}$. The position of VT 1210+4956 is consistent with the MAXI data and implies a short, fading burst that occurred at the beginning of the GSC's $\sim 40\text{-s}$ transit (Fig. 3) (11). We estimate a false alarm probability for the spatial association of $(1.2 \text{ to } 4.8) \times 10^{-3}$ (11). We performed several additional consistency checks: (i) that the shock properties of VT 1210+4956 were consistent with an explosion on the date of GRB 140814A, (ii) that the upper limits from contemporaneous optical observations did not rule out a stripped envelope supernova at the location of VT 1210+4956 and time of GRB 140814A, and (iii) that alternative classes of x-ray transients are not consistent with the observational data (11).

Our association of VT 1210+4956 with GRB 140814A implies that the x-ray emission had a peak 2- to 10-keV luminosity of $\sim 4 \times 10^{46} \text{ erg/s}$. This combination of high luminosity, short duration, and soft spectrum is unlike other x-ray transients with measured luminosities. Known transients with similar spectral peaks and durations, such as the shock breakout of supernova SN 2008D (23), are more than three orders of magnitude less luminous. Transients with similar luminosities, such as x-ray flashes and low-luminosity GRBs, typically maintain this luminosity for at least an order of magnitude longer duration (24), or peak at one or more orders of magnitude higher energy (25). The luminosity and duration of MAXI 140814A implies a relativistic outflow with Lorentz

¹Division of Physics, Mathematics, and Astronomy, California Institute of Technology, Pasadena, CA 91125, USA. ²School of Physics and Astronomy, Tel Aviv University, Tel Aviv, 69978, Israel. ³Department of Astronomy, University of California, Berkeley, CA 94720, USA. ⁴Miller Institute for Basic Research in Science, Berkeley, CA 94720, USA.

⁵Department of Physics, University of Alberta, Edmonton, Alberta T6G 2E1, Canada. ⁶Research Center for the Early Universe, Graduate School of Science, University of Tokyo, Bunkyo-ku Tokyo 113-033, Japan. ⁷National Radio Astronomy Observatory, Socorro, NM 87801, USA. ⁸Racah Institute of Physics, The Hebrew University of Jerusalem, Jerusalem, 91904, Israel.

*Corresponding author. Email: dillondong@astro.caltech.edu

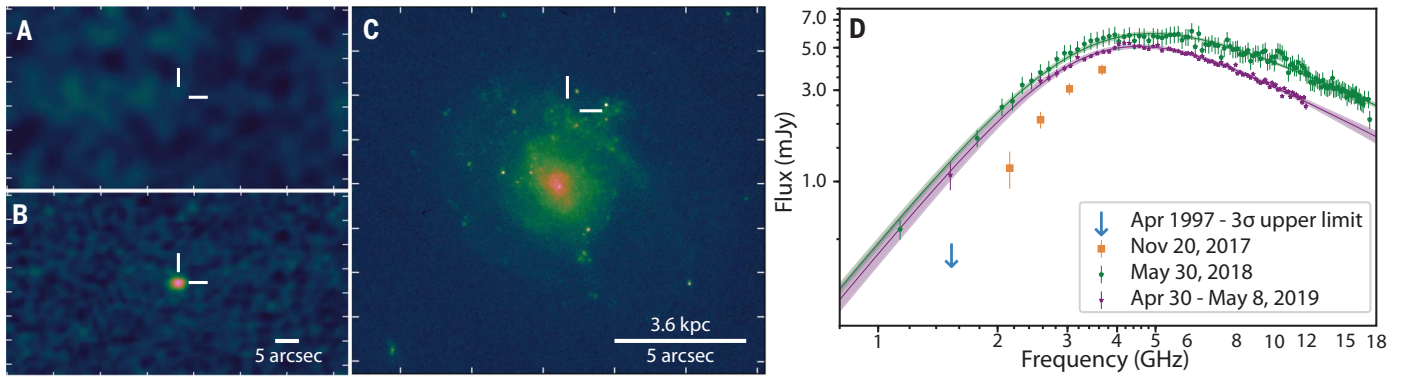
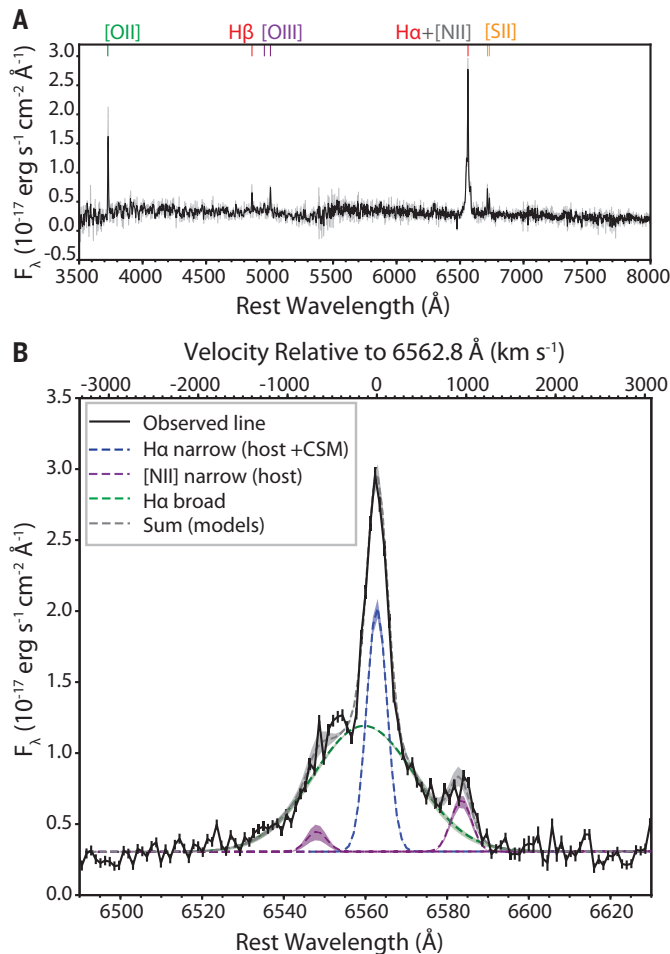


Fig. 1. The luminous radio transient VT 1210+4956. (A) Nondetection in the FIRST survey at 1.4 GHz, with a 3σ upper limit of 0.41 millijansky (mJy) on 17 April 1997. (B) Detection in VLASS at 3 GHz at 2.7 ± 0.1 (stat) ± 0.5 (sys) mJy on 20 November 2017, 20.59 years after the FIRST observation, at right ascension 12h10m01.32s, declination $+49^\circ56'47.006''$ [as indicated by white

crosshairs in (A) to (C)]. (C) Optical image of the location of VT 1210+4956 taken from the Hubble Space Telescope archive (PI: T. Schrabback). (D) Radio spectrum of VT 1210+4956 measured from the VLASS observation and follow-up epochs observed with the VLA, plotted with 1σ uncertainties. Follow-up epochs are fitted with a synchrotron self-absorption model (11).

Fig. 2. Optical spectrum of VT 1210+4956.

Image taken with Keck/LRIS on 13 April 2018, ~ 4.45 months after the detection in VLASS. (A) The full spectrum, including spectrally unresolved emission lines from the host galaxy. Unbinned data are shown in gray; data shown in black were smoothed with a $3\text{-}\text{\AA}$ boxcar kernel. (B) Details of the H α and [NII] part of the spectrum, with Gaussian models fitted to the lines. The narrow H α and [NII] lines are unresolved, whereas the broad component has a full width at half maximum of 1340 ± 60 km/s. The best-fitting model parameters and their uncertainties are listed in table S1.



factor $\gamma \geq 2.5$, and the characteristic energy of the photons implies a jetted geometry (11). Producing such a relativistic jet requires the presence of a central engine at the time of explosion.

Unlike the early relativistic jet, the radio emission detected in our follow-up epochs

(observed >3 years after GRB 140814A) was powered by a low-velocity shock propagating in a dense, extended CSM. The spectral peaks of the radio spectra are caused by synchrotron self-absorption rather than by free-free absorption, suggesting that the CSM is asymmetric, observed along a lower-density

line of sight (11). The peak luminosities and frequencies imply forward shock radii $R \sim 9 \times 10^{16}$ cm, postshock magnetic fields $B \sim 0.35$ G, and energies dissipated in the shock $U \sim 7 \times 10^{49}$ erg (11). The change in R between follow-up epochs implies a forward shock velocity of ~ 1800 km/s (11). This velocity, which is similar to the width of the broad H α line, implies a high density of $\sim 10^6$ cm $^{-3}$ for the CSM swept up in the ~ 1 year between follow-up epochs. This density is sufficient to allow the shocked gas to cool, on a time scale of ~ 1 year, from a shock-heated temperature of $\sim 10^7$ K to an $\sim 10^4$ K dense shell, cool enough to produce the H α emission (26). Compared with known explosive radio transients, VT 1210+4956 has a highly energetic shock propagating at low velocity and a high CSM density at large radius (Fig. 4).

Measurements of the CSM density as a function of radius trace the rate and timing of pre-explosion mass loss. Accounting for both the cool H α -emitting gas and the hot synchrotron-emitting gas, we found a lower limit to the total swept-up CSM mass of $\geq 1 M_\odot$ (11). The high density and total mass at a radius of $\sim 10^{17}$ cm requires a pre-explosion mass loss rate of $\dot{M} \approx 4 \times 10^{-2} (v/100 \text{ km s}^{-1}) M_\odot \text{ year}^{-1}$, where v is the preshock CSM velocity (11). This is more than an order of magnitude higher than the densest observed stellar winds and requires a pre-supernova eruption (27). With these observed and inferred constraints on the CSM velocity, we found that the eruption occurred a few centuries before the explosion (Fig. 4) (11).

Similar pre-explosion eruptive mass loss has been inferred from the dense and extended CSM around a few peculiar supernovae, including SN 2014C (28–30) and SN 2001em (31, 32), which both transitioned from stripped envelope (type Ib/c) to interacting (type II n) spectral classifications. Several models have

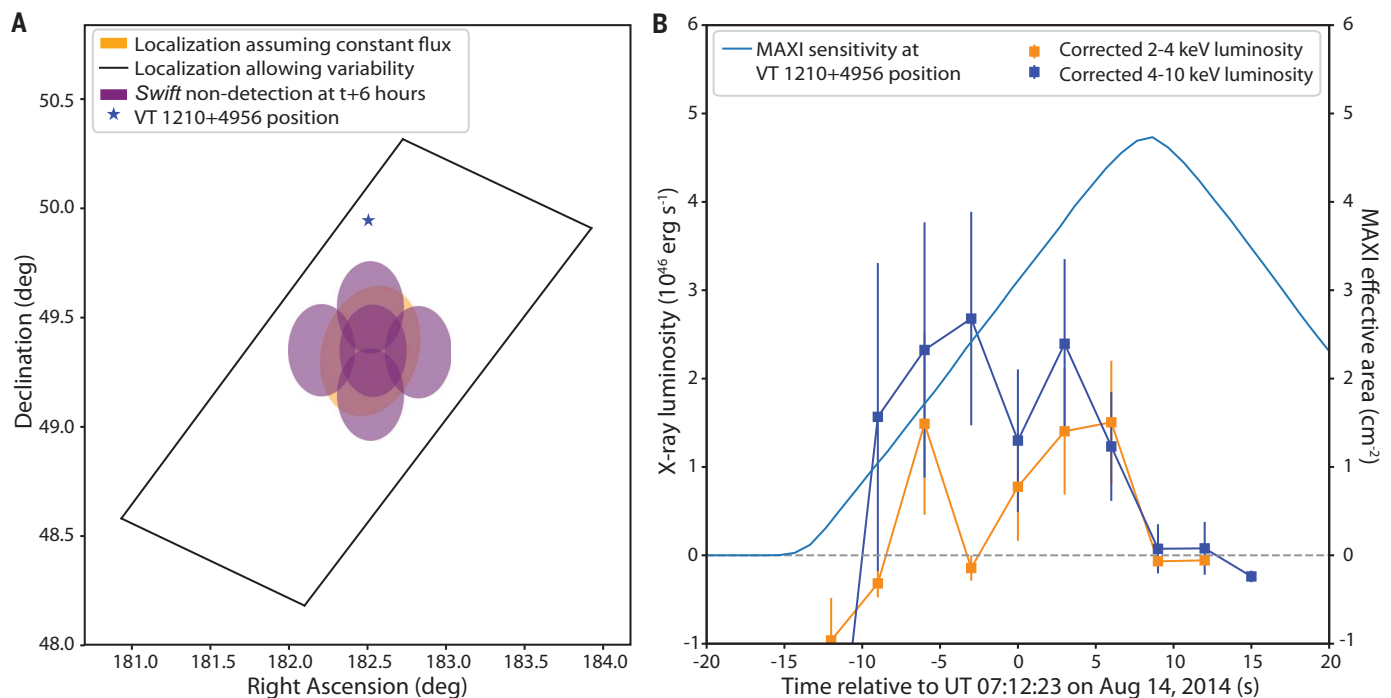


Fig. 3. The x-ray transient MAXI 140814A, which we associate with VT 1210+4956, was observed 3.268 years before VLASS detection. (A) Location of VT 1210+4956 compared with published MAXI localizations. Orange ellipse assumes constant flux and black rhombus allows for variability. This position is consistent within 1σ of the expectation

from the light curve in (B) (II). The purple ellipses show fields with nondetections in Swift observations, with upper limits 60,000 times fainter than the MAXI 140814A ~ 6 hours after the burst (II). (B) MAXI 2- to 4-keV (orange) and 4- to 10-keV (blue) light curves, corrected for instrumental sensitivity at the location of VT 1210+4956 (II).

been proposed to explain the synchronization of this eruptive mass loss with core collapse, including nuclear burning instabilities (28, 33), binary interaction timed coincidentally with core collapse (28, 30), and merger-driven explosions (6, 7, 28). For VT 1210+4956, the detection of a central engine allowed us to distinguish between these scenarios, and the order-of-magnitude higher radio luminosity and shock energy suggests the possibility of a different origin to SN 2014C and SN 2001em.

Nuclear burning instabilities strong enough to produce VT 1210+4956's pre-explosion mass loss rate are predicted to occur in only the final few years before core collapse (33), so they would produce shells that are more than an order of magnitude more compact at the time of interaction than we observed. Binary mass transfer is common in massive stars and is more consistent with the early eruptive mass loss. Approximately 70% of massive stars are found in orbits that will eventually lead to mass transfer, with an estimated third of these interactions leading to common envelope inspiral (1, 2). Such interactions are predicted to drive mass loss at or above the rate inferred for VT 1210+4956 (27). Unlike the case in single-star models, the mass is ejected in the plane of the binary (4, 7), providing a natural explanation for the inferred asymmetry of the CSM.

Binary interactions can occur at any time during the life of a star and can thus produce shells at any radius. However, the delay time

between eruption and core collapse constrains the specific type of interaction. At the near solar metallicity of VT 1210+4956's host galaxy, most interactions are expected to occur while the mass donor is undergoing fusion of hydrogen or helium, $\sim 10^4$ to 10^7 years before core collapse (34). Interactions synchronized coincidentally within $\sim 10^2$ years of core collapse are expected to be extremely rare (34), although uncertainties in the rates from binary population synthesis modeling allow this to be a viable scenario for previous events such as SN 2014C (28, 30).

The synchronization is more naturally explained if the interaction itself triggers the core collapse. To do so, an inspiraling object must disrupt the donor star's core. A non-compact merging body (e.g., a main sequence star) is unable to do so because it would replenish fuel in the core, producing a rejuvenated massive star (35). By contrast, an inspiraling neutron star or black hole is capable of tidally disrupting the core, leading to a merger-driven explosion (6, 7). During the inspiral phase, the compact object is expected to eject mass from the donor star at a rate similar to our calculated value (36). When it reaches the core, theory predicts the formation of an accretion disk and launching of a jet (6, 7). Of the models that we considered for eruptive mass loss, this scenario is most consistent with the jetted x-ray transient.

The high mass loss rate that we infer occurred centuries before explosion, much longer than

the dynamical time scale of the inspiraling compact object, which may indicate that the donor star had an envelope with a steep density profile. This would be theoretically expected for a star undergoing core helium fusion, for example (36). A steep density profile is thought to be required for merger during the dynamical inspiral phase (36, 37). Flatter density profiles would lead to full envelope ejection before merger, producing close compact object-evolved star binaries. These binaries may subsequently evolve into double compact object systems, with orbits close enough to merge within the lifetime of the Universe, and therefore contribute to gravitational wave events (5, 36, 37). Our proposed scenario for VT 1210+4956 is an alternative outcome to the formation of such systems.

On the basis of our blind search, we estimate a rate of $(1 \text{ to } 8) \times 10^{-8} \text{ Mpc}^{-3} \text{ year}^{-1}$ for transients with similar 3-GHz luminosities to VT 1210+4956 (II). However, given the continuous distributions of stellar binary periods and mass ratios (1, 2), there may be a wider range of delays between interaction and core collapse, thus producing CSM shells at smaller or larger radii. If this is the case, then these events may be more easily identified at other frequencies, so we regard this rate as a lower limit on the rate of merger-driven explosions.

REFERENCES AND NOTES

1. H. Sana et al., *Science* **337**, 444–446 (2012).
2. M. Moe, R. Di Stefano, *Distribution of Binary Stars. Astrophys. J. Suppl. Ser.* **230**, 15 (2017).

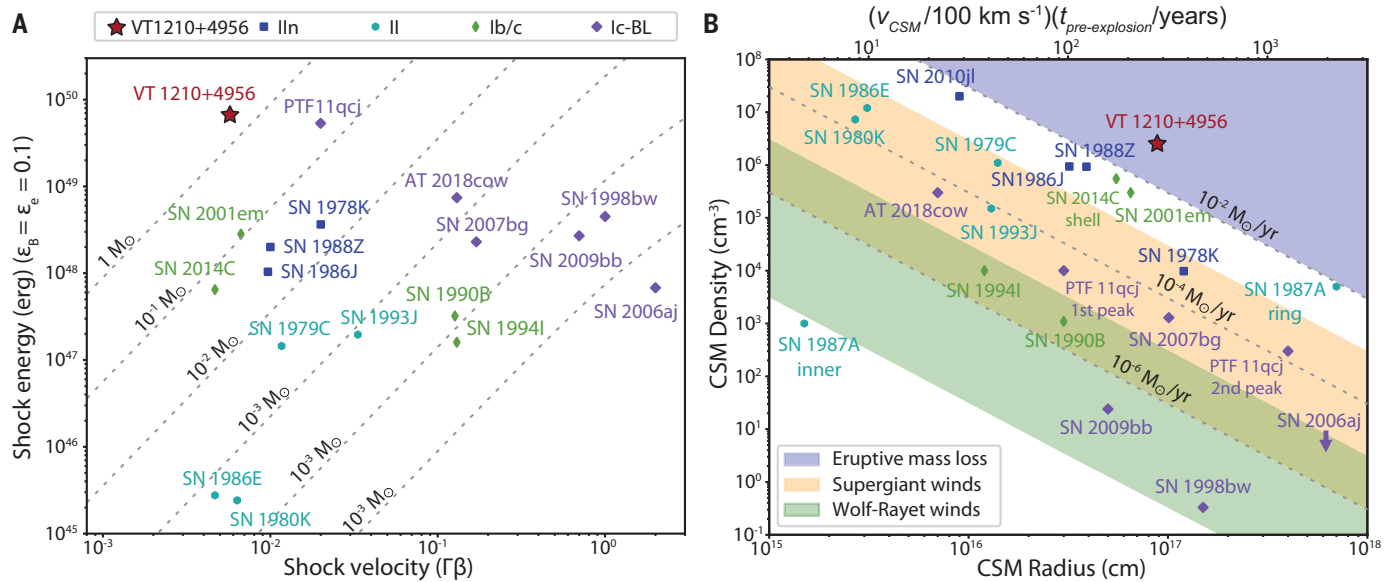


Fig. 4. Comparison of inferred shock properties for VT 1210+4956 and other luminous radio supernovae. (A) Shock energies derived from broadband radio spectra versus shock velocities. The dashed curves show constant shocked mass, assuming that the shock energy is equal to the kinetic energy. **(B)** CSM density versus CSM radius with values derived from optical and radio spectra.

The upper axis gives the time between mass loss and explosion normalized to a CSM velocity of 100 km/s. The dotted and dashed lines indicate constant mass flow rates M/v , with the color-shaded regions indicating approximate ranges of values for winds and eruptive mass loss from different types of systems (27). Sources are listed in table S5.

3. J. Orosz *et al.*, *Astrophys. J.* **742**, 84 (2011).
4. M. MacLeod, E. C. Ostriker, J. M. Stone, *Astrophys. J.* **868**, 136 (2018).
5. T. M. Tauris *et al.*, *Astrophys. J.* **846**, 170 (2017).
6. R. A. Chevalier, *Astrophys. J.* **752**, L2 (2012).
7. S. L. Schroder, M. MacLeod, A. Loeb, A. Vigna-Gómez, I. Mandel, *Astrophys. J.* **892**, 13 (2020).
8. N. Soker, *Mon. Not. R. Astron. Soc.* **471**, 4839–4843 (2017).
9. M. Lacy *et al.*, *Publ. Astron. Soc. Pac.* **132**, 035001 (2020).
10. R. H. Becker, R. L. White, D. J. Helfand, *Astrophys. J.* **450**, 559 (1995).
11. Materials and methods are available as supplementary materials.
12. D. S. Aguado *et al.*, *Astrophys. J. Suppl.* **240**, 23 (2019).
13. D. Milisavljevic *et al.*, *Astrophys. J.* **751**, 25 (2012).
14. K. Heng, *Publ. Astron. Soc. Aust.* **27**, 23–44 (2010).
15. R. A. Chevalier, *Astrophys. J.* **499**, 810–819 (1998).
16. A. J. van der Horst *et al.*, GRB 030329: 3 years of radio afterglow monitoring *Philos. Trans. A Math Phys. Eng. Sci.* **365**, 1241–1246 (2007).
17. A. Y. Q. Ho *et al.*, *Astrophys. J.* **871**, 73 (2019).
18. A. Y. Q. Ho *et al.*, *Astrophys. J.* **895**, 49 (2020).
19. A. Corsi *et al.*, *Astrophys. J.* **782**, 42 (2014).
20. S. R. Kulkarni *et al.*, *Nature* **395**, 663–669 (1998).
21. A. M. Soderberg *et al.*, *Nature* **463**, 513–515 (2010).
22. M. Serino *et al.*, *Publ. Astron. Soc. Jpn.* **66**, 87 (2014).
23. A. M. Soderberg *et al.*, *Nature* **453**, 469–474 (2008).
24. S. Campana *et al.*, *Nature* **442**, 1008–1010 (2006).
25. G. Ghirlanda, M. G. Bernardini, G. Calderone, P. D’Avanzo, *J. High Energy Astrophys.* **7**, 81–89 (2015).
26. B. T. Draine, *Physics of the Interstellar and Intergalactic Medium* (Princeton Univ. Press, 2011).
27. N. Smith, *Annu. Rev. Astron. Astrophys.* **52**, 487–528 (2014).
28. R. Margutti *et al.*, *Astrophys. J.* **835**, 140 (2017).
29. G. E. Anderson *et al.*, *Mon. Not. R. Astron. Soc.* **466**, 3648–3662 (2017).
30. N. C. Sun, J. R. Maund, P. A. Crowther, *Mon. Not. R. Astron. Soc.* **497**, 5118–5135 (2020).
31. N. N. Chugai, R. A. Chevalier, *Astrophys. J.* **641**, 1051–1059 (2006).

32. P. Chandra, R. A. Chevalier, N. Chugai, D. Milisavljevic, C. Fransson, *Astrophys. J.* **902**, 55 (2020).
33. S. Wu, J. Fuller, *Astrophys. J.* **906**, 3 (2021).
34. J. Klencki, G. Nelemans, A. G. Istrate, O. Pols, *Astron. Astrophys.* **638**, A55 (2020).
35. N. Langer, *Annu. Rev. Astron. Astrophys.* **50**, 107–164 (2012).
36. R. E. Taam, E. L. Sandquist, *Annu. Rev. Astron. Astrophys.* **38**, 113–141 (2000).
37. N. Ivanova *et al.*, *Astron. Astrophys. Rev.* **21**, 59 (2013).
38. D. Z. Dong, dillon-z-dong/vt1210: initial release, version 1.0, Zenodo (2021); <https://doi.org/10.5281/zenodo.5136735>.

ACKNOWLEDGMENTS

We thank the NRAO staff who made the VLASS possible, the VLASS Survey Science Group, J. Fuller and J. Lux for useful discussions, and the reviewers for helpful comments. Our results are based on data from the Karl G. Jansky Very Large Array, which is operated by the National Radio Astronomy Observatory (NRAO). The NRAO is a facility of the National Science Foundation operated under cooperative agreement by Associated Universities Inc. This research has made use of MAXI data provided by RIKEN, JAXA, and the MAXI team. Some of the data were obtained at the W. M. Keck Observatory, which is operated as a scientific partnership among the California Institute of Technology, the University of California, and the National Aeronautics and Space Administration. Keck Observatory was made possible by the generous financial support of the W. M. Keck Foundation. We recognize and acknowledge the cultural role and reverence that the summit of Maunakea has always had within the indigenous Hawaiian community. We are most fortunate to have the opportunity to conduct observations from this mountain. **Funding:** D.Z.D. and G.H. were supported by National Science Foundation (NSF) grant AST-1654815. G.H., D.Z.D., and A.H. were supported by the United States–Israel Binational Science Foundation (grant 2018154). A.H. also acknowledges support from the I-Core Program of the Planning and Budgeting Committee and the Israel Science Foundation and ISF grant 647/18. A.Y.Q.H. and K.D. were supported by the GROWTH project funded by the NSF under PIRE grant 1545949. A.K.H. was supported by NSERC Discovery

Grants RGPIN-2016-06569 and RGPIN-2021-04001. A.Y.Q.H. was supported by the Miller Institute for Basic Research in Science at the University of California, Berkeley. K.H. was supported by JSPS Early-Career Scientists grant 20K14513. S.M. was supported by the NRAO. S.R.K. was supported by the Heising-Simons Foundation. **Author contributions:** G.H., D.Z.D., and K.P.M. designed the transient search strategy. D.Z.D. implemented the transient search pipeline, with help from A.K.H. in visual vetting and A.Y.Q.H. in matching the MAXI transient. D.Z.D., G.H., and S.T.M. obtained the radio and optical follow-up observations with the help of telescope staff at the VLA and Keck. D.Z.D. processed and analyzed the radio data with contributions from S.T.M. D.Z.D. processed and analyzed the optical data and estimated the transient rates. E.N. led the analysis of the x-ray data with help from D.Z.D. D.Z.D. and G.H. wrote the paper with contributions from E.N., K.H., and the remaining authors. **Competing interests:** The authors declare no competing interests. **Data and materials availability:** VLASS quicklook images are available at <https://archive-new.nrao.edu/vlass/quicklook/>. VLA follow-up observations are available from the VLA archive at <https://archive.nrao.edu/> under project code 19A-422. The FIRST data were taken from <https://third.ucllnl.org/cgi-bin/firstcutout>. The Keck observations are available at https://koa.ipac.caltech.edu/cgi-bin/KOA/nph-KOALogin?more=with_KOALDs beginning LB.20180413. The Hubble Space Telescope image was taken from the archive <https://hla.stsci.edu/> under proposal ID 13493. Our analysis and model fitting software code is available at <https://github.com/Dillon-Z-Dong/VT1210> and is archived on Zenodo (38).

SUPPLEMENTARY MATERIALS

science.sciencemag.org/content/373/6559/1125/suppl/DC1
Materials and Methods
Supplementary Text
Tables S1 to S5
References (39–94)

15 January 2021; accepted 3 August 2021
10.1126/science.abg6037

A transient radio source consistent with a merger-triggered core collapse supernova

D. Z. DongG. HallinanE. NakarA. Y. Q. HoA. K. HughesK. HotokezakaS. T. MyersK. DeK. P. MooleyV. RaviA. HoreshM. M. KasliwalS. R. Kulkarni

Science, 373 (6559), • DOI: 10.1126/science.abg6037

Radio evidence of a stellar merger

Core collapse supernovae occur when a massive star exhausts its fuel and explodes. Theorists have predicted that a similar explosion could occur if an evolved massive star merges with a compact companion, such as a neutron star. Dong *et al.* have identified a radio source that was not present in earlier radio surveys. Follow-up radio and optical spectroscopy show that it is an expanding supernova remnant slamming into surrounding material, probably ejected from the star centuries before it exploded. An unidentified x-ray transient occurred at a consistent location in 2014, suggesting an explosion at that time that produced a jet. The authors suggest that the most likely explanation is a merger-triggered supernova. —KTS

View the article online

<https://www.science.org/doi/10.1126/science.abg6037>

Permissions

<https://www.science.org/help/reprints-and-permissions>

Use of this article is subject to the [Terms of service](#)

Science (ISSN) is published by the American Association for the Advancement of Science. 1200 New York Avenue NW, Washington, DC 20005. The title *Science* is a registered trademark of AAAS.

Copyright © 2021 The Authors, some rights reserved; exclusive licensee American Association for the Advancement of Science. No claim to original U.S. Government Works